Modeling for Batch Phenol Biodegradation with Immobilized *Alcaligenes faecalis*

Xiaoqiang Jia, Jianping Wen, Yan Jiang, Jing Bai, and Xianrui Cheng
Dept. of Biochemical Engineering, School of Chemical Engineering and Technology, Tianjin University, Tianjin 300072, P. R. China

Ying Zheng
Dept. of Chemical Engineering, University of New Brunswick, Fredericton, NB, Canada E3B 5A3

DOI 10.1002/aic.10744
Published online December 8, 2005 in Wiley InterScience (www.interscience.wiley.com).

Intrinsic cell growth and phenol biodegradation kinetics of Alcaligenes faecalis *were studied in shaking flasks. Batch phenol biodegradation experiments were carried out in a 7.5 L fermentor with immobilized* Alcaligenes faecalis *in polyurethane foams. A double-layer reaction-diffusion model was developed to describe the dynamic behaviors of batch phenol biodegradation processes. Phenol degradation (within the cell-immobilized polyurethane foams as well as in the main liquid phase) and cell growth (within the cell-immobilized polyurethane foams only) at different initial phenol concentrations were simulated and analyzed in terms of both biodegradation time and layer radius course. The good agreement between the model simulations and the experimental measurements for phenol degradation in the main liquid phase validates the proposed double-layer reaction-diffusion model.* © 2005 American Institute of Chemical Engineers *AIChE J,* 52: 1294–1303, 2006

Keywords: phenol biodegradation, immobilization, double-layer reaction-diffusion model

Introduction

Phenol and its homologues are very dangerous to the environment.[1] They come from forest fire, natural run-offs from urban areas where asphalt is used as binding material, natural decay of cellulosic materials, and industrial wastes derived from fossil fuel extraction and beneficiation processes, chemical manufacturing processes such as phenol manufacturing plants, pharmaceutical industry, wood processing industry, and pesticide manufacturing plants.[2] Thus, wastewater streams containing such phenolic pollutants require proper treatment before being discharged.

Traditionally, chemical and physical processes were adopted for the removal of high concentration phenol in industrial wastewater.[3] However, these processes produced a large quantity of undesirable by-products, which accelerated the introduction of biological methods of phenol removal in wastewater management.[4] Activated sludge process was one of the most widely accepted biological systems for the treatment of phenolic wastes,[5] but the activated sludge processes were sensitive to the fluctuations in the phenolic load.[6] Thus, pure bacteria (*Achromobacter*, *Alcaligenes, Pseudomonas, Rhodococcus*, etc.), yeasts (*Candida*, *Rodotorula*, *Trichosporon*, etc.) and fungi (*Aspergillus, Fusarium, Graphium, Penicillium*, etc.*)* capable of utilizing phenolic compounds found in soil and water environments are being applied to control phenolic wastes in recent years.[7]

However, the use of free cells for wastewater treatment also involves some serious problems. For example, high phenol concentration often causes a wash out of microbial cells, thus leading to the breakdown of a continuous process.[8] Therefore, immobilization technology draws increasing attention towards

Correspondence concerning this article should be addressed to J. P. Wen at jpwen@tju.edu.cn.

phenol biodegradation, which has been proved to be very effective for the desired purpose with little sludge production.[9,10] Pai et al.[11] performed continuous degradation of phenol using *Rhodococcus* sp. immobilized on granular activated carbon and on calcium alginate. Their work showed that the phenol removal rate was higher on alginate beads than on granular activated carbon at a fixed phenol influent but the granular activated carbon was more stable in providing consistent cellular activity when DO and pH fluctuated. Chen et al.[12] conducted continuous phenol degradation experiments by immobilized growing cells of *Candida tropicalis* entrapped into polyacrylamide gel beads. They found that the immobilization technique could enhance the tolerance ability of the yeasts to the phenol concentration up to 4000~5000 mg/L to achieve a phenol removal efficiency of over 95%. Chung et al.[8] compared the phenol degradation and cell growth kinetics of the free *Pseudomonas putida* CCRC 14365 and the Ca-alginate gel-immobilized one. Their results revealed that the immobilized cells could tolerate a much higher level of phenol load than the free cells. Quan et al.[13] immobilized *Achromobacter* sp. in an airlift bioreactor packed with honeycomb ceramic carriers and then performed fed-batch and continuous operations with mixed substrates of phenol and 2,4-dichlorophenol (2,4-DCP). It was reported that such immobilized strains could efficiently degrade both phenol and 2,4-DCP. Erhan et al.[14] prepared highly porous micro-cellular polymers (MCP) particles with interconnecting micro-pores for the immobilization of *Pseudomonas syringae* for the degradation of phenol in a fixed-bed column bioreactor with the aim of increasing bacterial population in the support through the provision of oxygen and nutrient to the interior of the support. It was found that phenol was degraded only on the surface of the MCP support after the complete coverage of the MCP support particles with biofilm.[14,15]

However, few studies have been carried out to model the dynamic behaviors of the phenol biodegradation and cell growth of the immobilized systems. Banerjee et al.[16] presented a reaction-diffusion model to analyze the mass transfer limitations in phenol biodegradation using *Pseudomonas putida* immobilized in spherical calcium alginate beads. The extent of mass transfer limitations under the conditions, including initial substrate concentration, cell loading, gel bead size, and loading density, was investigated through this model simulations. As far as we know, studies of the double-layer reaction-diffusion model on the dynamic behaviors of phenol biodegradation processes with immobilized *Alcaligenes faecalis* in polyurethane foams have not been documented.

The objective of this work is to investigate the phenol biodegradation with immobilized *Alcaligenes faecalis* in polyurethane foams at different initial phenol concentrations and to develop a double-layer reaction-diffusion mathematical model to predict the dynamic behaviors of batch phenol biodegradation processes.

Materials and Methods

Microorganism

Alcaligenes faecalis was isolated from acclimated activated sludge, which was collected from a municipal gasworks in China. This isolated activated sludge was then enriched for 10 weeks using phenol as the sole carbon source in synthetic mineral medium. The bacteria were isolated using shaking flask enrichment by the dilution method. Appropriately diluted activated sludge was inoculated into shaking flasks with LB medium and mineral salt medium, and its initial pH value was adjusted to 7.2. To obtain pure culture, the cells were transferred onto the agar plates containing 18 g agar per liter medium and then incubated at 30°C for about 18 h in a biochemical incubator. A dominant colony was purified by repeating the above transfers five times. Stock cultures of the bacteria were maintained by periodic sub-transfer on nutrient agar slants and stored at 4°C in the refrigerator. Liquid cultures were grown in the mineral salt medium supplemented with 500 mg/L phenol at 30°C in a rotary shaker at a shaking speed of 200 rpm. The strain was identified by the Institute of Microbiology, Chinese Academy of Sciences, Beijing, P. R. China. Identification studies on the strain revealed that the bacteria were *Alcaligenes faecalis.* Pure culture of *Alcaligenes faecalis* was used throughout this work.

Composition of growth medium

The liquid mineral salt medium contained (g/L): 0.4 K_2HPO_4, 0.2 KH_2PO_4, 0.1 NaCl, 0.1 $MgSO_4$, 0.01 $MnSO_4 \cdot H_2O$, 0.01 $Fe_2(SO_4)_3 \cdot H_2O$, 0.01 $Na_2MoO_4 \cdot 2H_2O$, 0.4 $(NH_4)_2SO_4$. Phenol was filter-sterilized through membranes (pore size of 0.2 μm) and added to the medium before inoculation.[17,18]

Analytical procedures

Cell density in shaking flasks was monitored spectrophotometrically by measuring the absorbance at the wavelength of 600 nm. Biomass concentration on a dry weight basis was measured by filtering the cell suspension with a filter and drying the filter paper and cells to a constant weight for 24 h at 80°C. For batch phenol biodegradation in the fermentor, the fermentation broth was sampled periodically to measure the broth concentrations of phenol. The concentration of residual phenol was measured using high-performance liquid chromatography (HPLC, model Series III, LabAlliance) equipped with a C18 column (250 × 4.6 mm, LabAlliance, USA). The absorbance of the effluent solution was continuously measured at 280 nm. The flow rate was 1.0 mL/min and the mobile phase was 57.1% (V/V) of methanol. The culture broth was centrifuged at 10,000×g for 8 min, and the supernatant was analyzed. The retention time of phenol was 5.04 min. To measure the concentration of the immobilized cell density, predetermined numbers (usually 10) of the cell-immobilized polyurethane foams were sampled. After thoroughly washing with deionized water, the polyurethane foams were dried at 80°C after 24 h to determine the dry cell weight. All the experiments were performed in triplicate, and the average error was within ±5%.

Intrinsic kinetics

The startup of the experiments was obtained by inoculating 10 mL LB medium with *Alcaligenes faecalis* from nutrient agar slants stored in a 4°C refrigerator, in sterile conditions. After 18 h of incubation at 30°C, 2 mL of this cell culture was added to 100 mL fresh LB medium with the same phenol concentra-

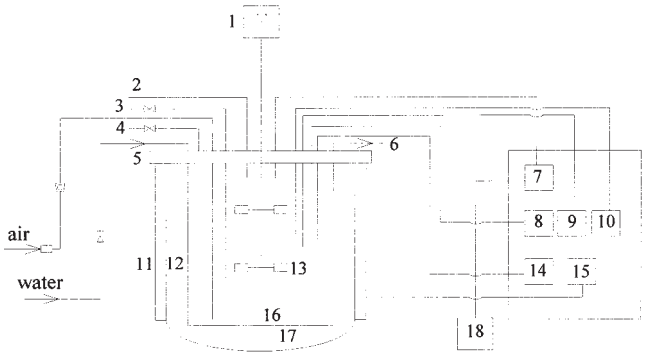

Figure 1. Diagram of the apparatus.

(1) Agitation motor, (2) exhaust tube, (3) harvest tube, (4) sample point, (5) water inlet, (6) water outlet, (7) pump control, (8) pH control, (9) DO control, (10) temperature control, (11) blanket heater, (12) vessel, (13) agitation impellor, (14) level control, (15) heater, (16) ring sparger, (17) cooling coil, (18) addition bottle.

tion as inoculums. About 7 h later, optical density of cells grown in the metaphase of exponential stage was monitored.

For the determination of the kinetic parameters, 5 mL subculture was used to inoculate into 250 mL shaking flasks containing 50 mL sterile mineral salt medium with an initial phenol concentration over the range from 100 to 1600 mg/L at 100 mg/L intervals. Samples were periodically taken for the measurements of cell and phenol concentrations. All of the above experiments were carried out at the initial pH of 7.2 and temperature of 30°C in an orbital shaker at a shaking speed of 200 rpm.

Immobilization

The physical properties of the polyurethane foams used in the immobilization procedure are as follows: apparent density of 50 kg/m^3, porosity of 90%, average pore size of 0.3 mm. *Alcaligenes faecalis* was attached to 5 mm polyurethane foam cubes by a two-step immobilization procedure. First, 130 mL LB medium in a 500 mL flask was autoclaved together with 25 mL of the polyurethane foam cubes. Then the bacteria were inoculated and incubated in an incubation shaker for cell immobilization. After 22 h, the nutrients were exhausted and the cell-immobilizing polyurethane foams were transferred to another flask containing 130 mL fresh LB medium for another 8 h. The cultures were maintained at 30°C and a shaking speed of 200 rpm. Finally, the cell-immobilized matrix was thoroughly washed with the sterilized deionized water three times to remove any residual medium. Thus, the immobilized *Alcaligenes faecalis* in polyurethane foams were obtained, and were further used in the following batch phenol biodegradation experiments and theoretical studies.

Batch phenol biodegradation in fermentor

The 7.5 L fermentor (BioFlo 110, New Brunswick Scientific Co., Inc.) is shown in Figure 1. The fermentor was sterilized with 3% hydrogen peroxide solution and washed with sterilized deionized water prior to fermentation experiments. For each batch phenol biodegradation process, after washing with deionized water and sterilized mineral salt medium, 3 L mineral salt medium containing different initial phenol concentrations and a certain volume of the cell-immobilized polyurethane foams with the solid loading ε of 7.5×10^{-3} L/L was added into the fermentor. All of the experiments were carried out at the initial pH of 7.2 and at an agitation speed of 450 rpm. The fermentation temperature was kept at 30°C by circulating thermostated water in the water jacket. The fermentation broth was sampled periodically to measure the broth concentrations of phenol.

Theory

Mathematical model

It is very important to evaluate the cell distribution within the cell-immobilized polyurethane foams. First, an electric light source microscope (ELSM) was used to take the photograph of the cross section of the stained cell-immobilized matrix, as shown in Figure 2. It is noted that there are two layers existing. The inner core is hard to be stained because of no bacteria existing, while the surface layer could be stained into purple due to the presence of hundreds of thousands of bacteria. Second, the photograph of the cross section of the cell-immobilized matrix was taken by scanning electron microscope (SEM) to determine the thickness of the surface layer where bacteria accumulate, and the result is illustrated in Figure 3. It is clear that the surface layer becomes very dense because of cell accumulation and the thickness of the surface cell-grown layer is about 0.3 mm, while the equivalent radius of the cell-immobilized polyurethane foams is 2.5 mm.

Based on the ELSM and SEM observations for the cell-immobilized polyurethane foams, it can be concluded that there are two layers within the cell-immobilized polyurethane foams. That is, the surface layer is for cell growth and phenol biodegradation—the surface diffusion-reaction layer; while the inner core embraced by the surface layer is for substrate and product diffusions only—the inner diffusion layer, as shown in Figure 4.

A double-layer reaction-diffusion model is proposed to predict the dynamic behaviors of batch phenol biodegradation processes by immobilized *Alcaligenes faecalis* in polyurethane foams in the fermentor. Four assumptions are made:

Figure 2. The ELSM photograph of the cross section of the cell-immobilized polyurethane foam (25 × 4 folds).

[Color figure can be viewed in the online issue, which is available at www.interscience.wiley.com.]

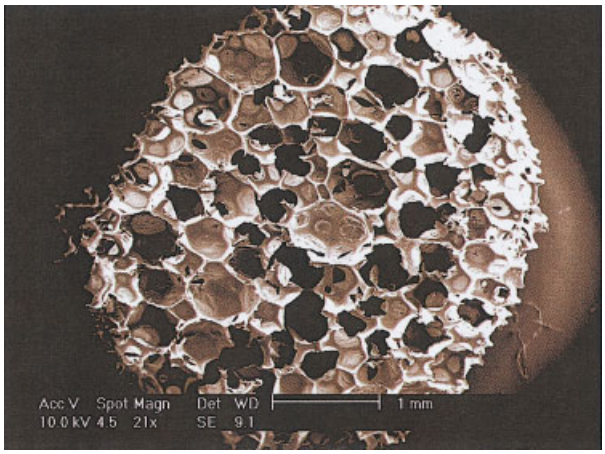

Figure 3. The SEM photograph of the cross section of the cell-immobilized polyurethane foam.

[Color figure can be viewed in the online issue, which is available at www.interscience.wiley.com.]

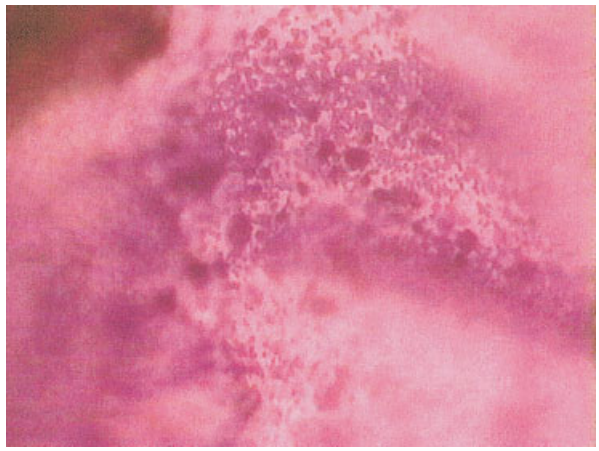

Figure 5. The ELSM photograph of a slice of the surface layer of the cell-immobilized polyurethane foam (25 × 40 folds).

[Color figure can be viewed in the online issue, which is available at www.interscience.wiley.com.]

(1) The main liquid phase in the fermentor is completely mixed and the phenol concentration is uniform in the main liquid phase.

(2) The initial bacteria are distributed uniformly in the surface diffusion-reaction layer. Moreover, to simplify the model development, the equivalent radius of the cell-immobilized polyurethane foams remains constant during fermentation.

(3) The influence of free cells in the main liquid phase is negligible.

(4) As the polyurethane foams are cell-immobilized ones before used in batch phenol biodegradation experiments in a stirred tank, and most space of the pores of the surface diffusion-reaction layer has been occupied by hundreds of thousands of small bacilli (about $0.5 \times 1.0\ \mu$m) as shown in Figure 5, the pore effects on surface diffusion and the pore diffusion are negligible according to the criterion proposed by Brooks et al.[19]

Thus, in view of the assumptions mentioned above, the mathematical model for the batch phenol biodegradation processes with the immobilized *Alcaligenes faecalis* in polyurethane foams can be developed as follows:

Mass balance for phenol in the inner diffusion layer:

$$\frac{\partial C_{S,1}}{\partial t} = D_{S,1}\left(\frac{\partial^2 C_{S,1}}{\partial r^2} + \frac{2}{r}\frac{\partial C_{S,1}}{\partial r}\right) \tag{1}$$

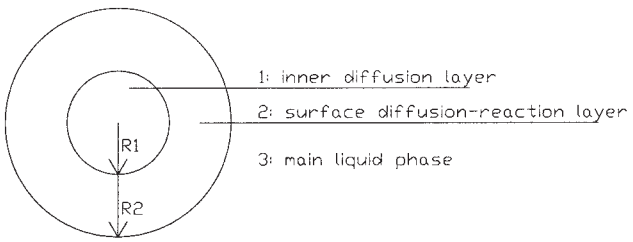

Figure 4. Diagram of the double-layer reaction-diffusion model.

Mass balance for phenol in the surface diffusion-reaction layer:

$$\frac{\partial C_{S,2}}{\partial t} = D_{S,2}\left(\frac{\partial^2 C_{S,2}}{\partial r^2} + \frac{2}{r}\frac{\partial C_{S,2}}{\partial r}\right) - \gamma_S \tag{2}$$

where γ_S is the phenol consumption rate. It is a function of phenol concentration and cell density, both of which are continually changing with time. $D_{S,1}$ and $D_{S,2}$ are the phenol diffusion coefficients in the inner core and the surface layer, respectively.

Mass balance for biomass in the surface diffusion-reaction layer:

$$\frac{\partial C_X}{\partial t} = \gamma_X = \mu_X C_X \tag{3}$$

where C_X is the cell density based on the volume of the cell-immobilized polyurethane foams, γ_X the cell growth rate, and μ_X the specific cell growth rate.

In addition, mass balance for phenol in the main liquid phase within the fermentor can be derived as:

$$\frac{dC_{S,3}}{dt} = -K_{L,S}a\varepsilon(C_{S,3} - C_{S,2}|_{r=R_2}) \tag{4}$$

where α is the surface area per unit volume of the cell-immobilized polyurethane foams, and ε is the volume of cell-immobilized polyurethane foams per unit effective bioreactor volume (L/L). $K_{L,S}$ is the liquid-solid mass transfer coefficient of phenol from the main liquid phase to the surface of the cell-immobilized polyurethane foams.

The initial and boundary conditions are:

$$t = 0, \qquad C_X = C_{X,0}, \qquad C_{S,1} = C_{S,2} = 0, \qquad C_{S,3} = C_{S,0} \tag{5}$$

$$r = 0, \qquad \frac{\partial C_{S,1}}{\partial r} = 0, \qquad \frac{\partial C_{S,2}}{\partial r} = 0 \tag{6}$$

$$r = R_1, \qquad D_{S,1} \left.\frac{\partial C_{S,1}}{\partial r}\right|_{r=R_{1^-}} = D_{S,2} \left.\frac{\partial C_{S,2}}{\partial r}\right|_{r=R_{1^+}} \tag{7}$$

$$r = R_2, \qquad D_{S,2} \left.\frac{\partial C_{S,2}}{\partial r}\right|_{r=R_2} = K_{L,S}(C_{S,3} - C_{S,2}|_{r=R_2}) \tag{8}$$

where the initial cell density in the surface diffusion-reaction layer $C_{X,0}$ can be calculated as:

$$C_{X,0} = \frac{\overline{C_{X\,0}}}{1 - \left(\frac{R_1}{R_2}\right)^3} \tag{9}$$

with $\overline{C_{X\,0}}$ the experimentally determined average cell density in the whole cell-immobilized polyurethane foam.

Model parameters

To solve the above double-layer reaction-diffusion model, several model parameters, including intrinsic cell growth and phenol biodegradation kinetic parameters, phenol diffusion coefficients and liquid-solid mass-transfer coefficient of phenol from the main liquid phase to the surface of the cell-immobilized polyurethane foams, are needed.

Kinetic Parameters. Monod's model has been used extensively for the estimation of bio-kinetic constants for bacterial growth on non-inhibitory substrates. Due to the inhibitory effect of phenol, Haldane's equation was widely adopted to describe the kinetic behaviors for cell growth of phenol biodegradation processes[20,21]:

$$\mu_X = \frac{\gamma_X}{C_X} = \frac{1}{C_X}\frac{dC_X}{dt} = \frac{\mu_{\max} C_S}{K_s + C_S + \frac{C_S^2}{K_i}} \tag{10}$$

where $\mu_{\max}$ is the maximum specific growth rate, K_S the saturation constant, and K_i the inhibition coefficient.

Analyzing the utilization of substrate in cells, the consumption of substrate for growth and for maintenance, and also for product formation if possible, has to be considered.[22] The substrate consumption kinetics of phenol biodegradation is:

$$\gamma_S = -\frac{dC_S}{dt} = \frac{1}{Y_{X/S}}\gamma_X + mC_X + \frac{1}{Y_{P/S}}\gamma_P \tag{11}$$

where $\gamma_P = \alpha\gamma_X + \beta C_X$ is the product formation kinetics. As $Y_{X/S}$, m, $Y_{P/S}$, α, and β are all constants, Eq. 11 can be reduced to:

$$\gamma_S = A\gamma_X + B \cdot C_X \tag{12}$$

which can be reduced to the following equation divided by C_X:

$$\mu_S = \frac{\gamma_S}{C_X} = A\mu_X + B \tag{13}$$

The kinetic variables of cell growth and phenol biodegradation, including $\mu_{\max}$, K_S, K_i, A, and B, are regressed from the experimental data in shaking flasks. Detailed discussion will be provided in the Results and Discussion section.

Diffusion Coefficients. The phenol diffusion coefficient in the inner core of the cell-immobilized polyurethane foams is close to that in the pure water because there are few cells in the inner core.[23] Banerjee et al.[16] reported that the phenol diffusion coefficient in the pure water $D_{S,1}$ is 2.34×10^{-6} m^2/h. The effective phenol diffusion coefficient in the surface diffusion-reaction layer is calculated using the random-pore model for phenol diffusion when cells exist[16,24]:

$$D_{S,2} = D_{S,1}(1 - 2.6 \times 10^{-3} C_X)^2 \tag{14}$$

Obviously, the effective phenol diffusion coefficient in the surface cell layer is a function of time, as C_X increases with time.

Mass-Transfer Coefficient. The liquid-solid mass-transfer coefficient of phenol from the main liquid phase to the surface of the cell-immobilized polyurethane foams in stirred-tank experiments is calculated using the following correlation, which is used for the calculation of mass-transfer coefficient from liquid phase to low-density solids in agitated dispersions[25]:

$$K_{L,S} = \frac{2D_S}{d_p} + 0.31\left(\frac{\mu}{\rho D_S}\right)^{-2/3}\left(\frac{\Delta\rho\mu g}{\rho^2}\right)^{1/3} \tag{15}$$

where D_S is the free diffusion coefficient of phenol in water, d_P the equivalent diameter of the polyurethane foam, μ the viscosity of the solution containing phenol, ρ the density of the continuous phase, and $\Delta\rho$ the density difference between the liquid phase and the solid phase. Because the maximum phenol concentration in our experiments is 1600 mg/L, corresponding to a very small phenol holdup (V/V), the differences between the liquid density and viscosity of the solution containing phenol and those of the mineral salt medium are negligible according to the correlations proposed by Escobedo et al.[26] Thus, the density and viscosity of mineral salt medium, which can be measured experimentally, are used as those of the solution in the calculation of the liquid-solid mass transfer coefficient.

Solution technique

The equations, together with their initial and boundary conditions, are solved by the finite element analysis method using the software package of Femlab with 56 base mesh elements and 339 extended mesh elements. Four sub-domains, corresponding to the phenol concentration within the inner diffusion layer, the phenol concentration within the surface diffusion-reaction layer, the cell concentration within the surface diffusion-reaction layer, and the phenol concentration in the main liquid phase, were simulated with 1-D coefficient form using weak solution.

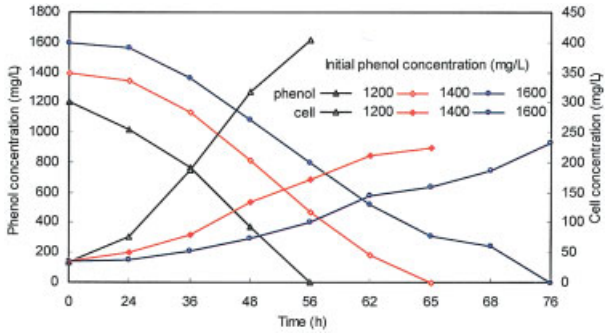

Figure 6. Phenol degradation and cell growth at different initial phenol concentrations in shaking flasks.

[Color figure can be viewed in the online issue, which is available at www.interscience.wiley.com.]

Results and Discussion

Intrinsic kinetics

Figure 6 shows the cell growth and phenol biodegradation in shaking flasks of *Alcaligenes faecalis* at three different initial phenol concentrations. With the increase of initial phenol concentration, the rate of phenol degradation velocity gradually decreases. It also reveals that bacteria undergo a longer lag phase at higher phenol concentration than lower phenol concentration.

The specific cell growth rates and specific phenol degradation rates are calculated using the experimental data. Using a nonlinear least-squares regression analysis by the software of Matlab, the Haldane's equation parameters are obtained using Eq. 10: $\mu_{max} = 0.13\ h^{-1}$, $K_S = 2.23$ mg/L, and $K_i = 239.4$ mg/L. The value of the squared 2-norm of the residual at these parameters (3.24×10^{-3}) is very small, indicating the regression curve agrees with the experimental data very well. Figure 7 presents the comparison between the kinetic simulations and the experimental data of cell specific growth rates at different initial phenol concentrations. From this Figure it can be seen that the regression curve agrees with the experimental data

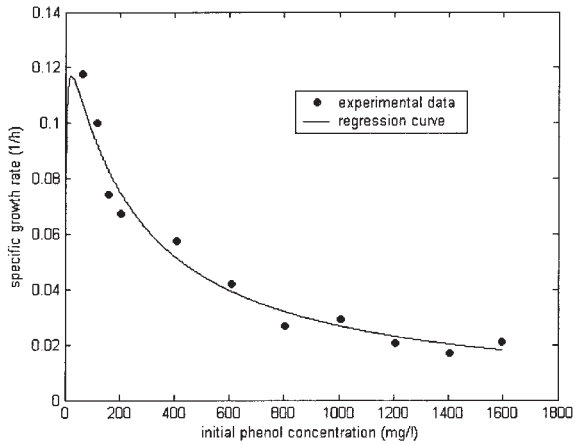

Figure 7. Comparison between model simulation and experimental determined specific cell growth rates of *Alcaligenes faecalis* at different initial phenol concentrations in shaking flasks.

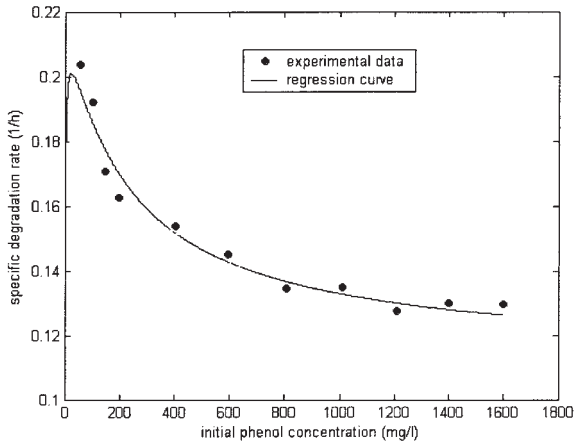

Figure 8. Comparison between model simulation and experimental determined specific phenol degradation rates of *Alcaligenes faecalis* at different initial phenol concentrations in shaking flasks.

quite well, as the correlation coefficient $R^2 = 0.97$ and the largest specific growth rate occurs at the phenol concentration of 77.9 mg/L. With further increase of phenol concentration, the substrate inhibition will increase, resulting in the decrease in the specific growth rates.

In addition, the phenol biodegradation parameters A and B are also regressed linearly using Eq. 13 on the basis of the experimental data of the specific cell growth rates and specific phenol biodegradation rates. $A = 0.756$ and $B = 0.113\ h^{-1}$ are obtained ($R^2 = 0.98$). The comparison between the simulated and the measured kinetic specific phenol biodegradation rates is shown in Figure 8. It can be seen that the simulated curve agrees well with the calculations based on the experimental data at different initial phenol concentrations ($R^2 = 0.96$).

The inner diffusion layer

To understand the dynamic behaviors of the immobilized system, the variations of substrate concentration and cell density in the cell-immobilized polyurethane foams are analyzed. In the inner diffusion layer, degradation of phenol is negligible due to no cells existing so that only diffusion of phenol is considered. Figure 9 illustrates the variations of phenol concentration at a fixed radial position of $r = 1.1$ mm with time course at different initial phenol concentrations. The cell-immobilized polyurethane foams are free of phenol when they are introduced into the system. Diffusion results in a sudden increase of phenol concentration inside the cell-immobilized polyurethane foams (the peak value appears around 1 h). As phenol builds up in the cell-immobilized polyurethane foams, the cells start growing in the surface diffusion-reaction layer. Therefore, phenol concentration starts to decrease in the surface diffusion-reaction layer, which leads to the transfer of phenol from the inner diffusion layer to the surface diffusion-reaction layer. After 30 hours, phenol concentrations almost drop to zero.

Figure 10 shows the variations of the predicted phenol concentration at six specified time points ($t = 0.05$, 0.5, 1.32, 5, 10, and 30 h, respectively) of the three regions (inner

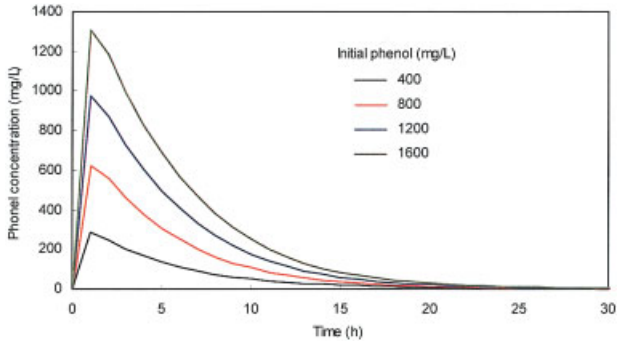

Figure 9. Time course of the changes of phenol concentration within the inner diffusion layer of the cell-immobilized polyurethane foams at different initial phenol concentrations of batch phenol biodegradation in fermentor (r = 1.1 mm).

[Color figure can be viewed in the online issue, which is available at www.interscience.wiley.com.]

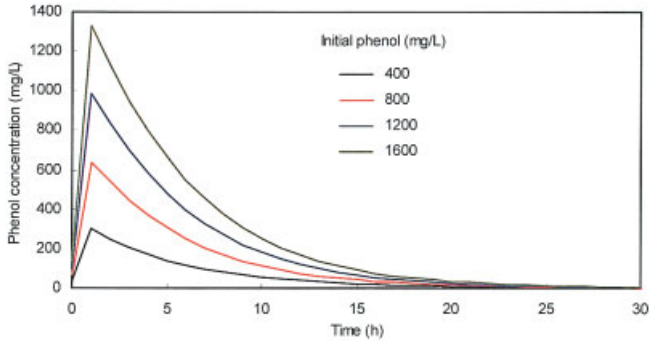

Figure 11. Time course of the changes of phenol concentration within the surface diffusion-reaction layer of the cell-immobilized polyurethane foams at different initial phenol concentrations of batch phenol biodegradation in fermentor (r =2.4 mm).

[Color figure can be viewed in the online issue, which is available at www.interscience.wiley.com.]

diffusion layer, surface diffusion-reaction layer, and main liquid phase) and the initial phenol concentration $C_{S,0}$ of 1600 mg/L. Lines of t = 0.05 h and t = 0.5 h indicate the inner diffusion layer has a lower phenol concentration compared to the surface diffusion-reaction layer at the beginning of the batch process, which makes phenol transfer from the surface diffusion-reaction layer to the inner diffusion layer. On the other hand, phenol begins to be consumed in the surface diffusion-reaction layer. The two opposite impacts make the phenol concentration reach its balance at the layer boundary, as shown by the line of t = 1.32 h. At this point, the phenol concentration is uniform within the entire cell-immobilized polyurethane foam. Beyond t = 1.32 h, the phenol concentration of the inner diffusion layer becomes higher than that of the surface diffusion-reaction layer due to the fact that the increased cell density consumes more phenol, bringing about the reversal of the phenol transfer direction, that is, from the inner diffusion layer to the surface diffusion-reaction layer, leading to the beginning of the decrease of phenol concentration with

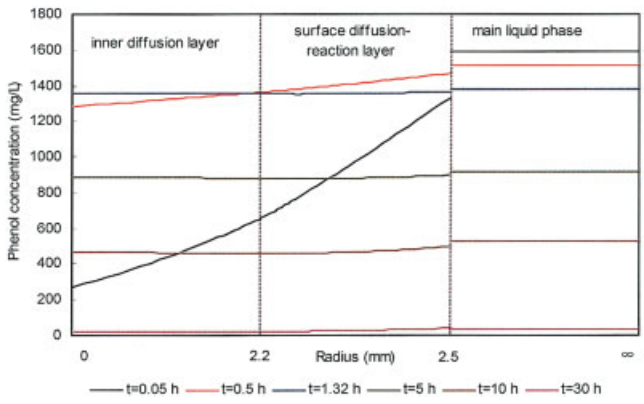

Figure 10. Radius course of the changes of phenol concentration in three regions at different time points of batch phenol biodegradation in fermentor ($C_{S,0}$ = 1600 mg/L).

[Color figure can be viewed in the online issue, which is available at www.interscience.wiley.com.]

radius course in the inner diffusion layer (line t = 5 h and line t = 10 h). However, after 30 hours, the phenol concentrations of the three regions all drop to almost nothing. Then no mass transfer exists.

The surface diffusion-reaction layer

In the surface diffusion-reaction layer, the phenol is consumed by the biomass. Figure 11 demonstrates the predicted phenol concentrations change against time within the surface diffusion-reaction layer at a fixed radial position of r = 2.4 mm and four initial phenol concentrations. It is seen that the phenol concentration in the surface diffusion-reaction layer follows a similar variation trend to the inner diffusion layer. But the concentration peaks are reached at different time points, which will be discussed in the next paragraph. An increase in the initial phenol concentration leads to a slower phenol reduction.

One could also draw the radius course of the phenol degradation process within the surface diffusion-reaction layer from Figure 10. As mentioned before, the mass transfer of phenol from the main liquid phase into the cell-immobilized polyurethane foams brings the buildup of phenol in both the inner and surface layers at the beginning of the process, as line t = 0.05 h shows. The cell growth within the surface diffusion-reaction layer provides a negative effect on phenol concentration compared to the mass transfer from the main liquid phase into the surface diffusion-reaction layer, making the peak value of phenol concentration appear a little earlier than that of the inner diffusion layer (line t = 0.5 h). Phenol is still transferred from the surface diffusion-reaction layer into the inner diffusion layer until the equilibrium occurs (line t = 1.32 h). After that time point, the phenol concentration of the surface diffusion-reaction layer becomes lower than that of the inner diffusion layer because of the increase of the cell density (line t = 5 h and t = 10 h). Note that the phenol concentration of the main liquid phase is always larger than that of the surface diffusion-reaction layer then phenol is transferred from the former into the later. Then there are three factors affecting the phenol concentration of the surface diffusion-reaction layer, that is, mass transfer from the main liquid phase into the surface

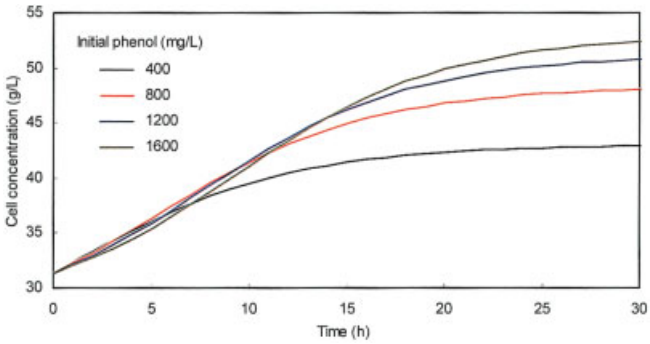

Figure 12. Time course of the changes of cell concentration within the surface diffusion-reaction layer of the cell-immobilized polyurethane foams at different initial phenol concentrations of batch phenol biodegradation in fermentor (r =2.4 mm).

[Color figure can be viewed in the online issue, which is available at www.interscience.wiley.com.]

diffusion-reaction layer (positive effect), mass transfer from the inner diffusion layer into the surface diffusion-reaction layer (positive effect), and cell consumption within the surface diffusion-reaction layer (negative effect). To estimate the relative magnitude of the two positive effects, a Biot number is defined:

$$Bi = \frac{K_{L,S}R}{D_{S,1}} \tag{16}$$

where $D_{S,1}$ is the diffusion coefficient of phenol within the inner diffusion layer, $K_{L,S}$ the liquid-solid mass transfer coefficient of phenol from the main liquid phase to the surface diffusion-reaction layer, and R the equivalent radius of the cell-immobilized polyurethane foams. When $Bi > 1$, the mass transfer from the main liquid phase into the surface diffusion-reaction layer plays the bigger part in the buildup of phenol within the surface diffusion-reaction layer. As can be seen in lines $t = 5$ h and $t = 10$ h, the interface between the surface diffusion-reaction layer and the main liquid phase has a higher phenol concentration compared with the interface between the surface diffusion-reaction layer and the inner diffusion layer due to a high Bi value (computed $Bi = 186$ by Eq. 16), resulting in the increase of phenol concentration with radius course within the surface diffusion-reaction layer. However, as substrate is further consumed, phenol concentrations in all three regions decrease with time course, and the differences between the surface diffusion-reaction layer and the other two regions become much smaller. Then phenol concentration in the surface layer as well as the other two regions reaches another equilibrium and then reduces to almost zero beyond 30 hours (line $t = 30$ h).

The change of cell concentration within the surface diffusion-reaction layer with time course predicted by the developed model is shown in Figure 12 for a given radial position of $r =$ 2.4 mm. Initially, cell growth rate of the low initial phenol concentration is faster than that of the high initial phenol concentration because of the substrate inhibition, corresponding to the highest cell concentration occurring at the lowest initial phenol concentration (400 mg/L). However, after a certain time, phenol is consumed to the extent that the substrate inhibition effect becomes weaker compared to the carbon source provision effect. Then the cell growth rate of the low initial phenol concentration becomes lower than that of the high initial phenol concentration because of the lack of carbon source. Finally, the lowest cell concentration occurs at the lowest initial phenol concentration (400 mg/L). For each initial phenol concentration, the cell concentration increases until phenol concentration falls to a low value. As fermentation proceeds further, phenol concentrations within the surface diffusion-reaction layer decrease to a certain extent and start limiting the growth of the cells, leading to the cell density not changing.

Figure 13 illustrates the predicted change of cell concentration within the surface diffusion-reaction layer at the initial phenol concentration of $C_{S,0} = 1600$ mg/L. It can be observed that at the beginning of the processes, cell concentration remains almost the same at different radius positions (line $t =$ 0.05 h). When the fermentation time varies from 0.5 h to 10 h, the cell density within the surface diffusion-reaction layer slightly decreases with increase in the radius course. This may be attributed to the fact that the increase of phenol concentration with increase in the radius course (as shown in Figure 10) brings about the enhanced substrate inhibition for phenol concentrations larger than 77.9 mg/L. However, as the batch process proceeds, with fermentation time increasing up to 30 h, corresponding phenol concentration is smaller than 77.9 mg/L within the surface diffusion-reaction layer and phenol concentration starts becoming a limiting factor of cell growth. Then the cell growth rate at the interface between the surface diffusion-reaction layer and the main liquid phase becomes higher than that at the two-layer boundary because of computed $Bi >$ 1. This results in the increase of the cell concentration at the outer edge of the surface layer as the batch process is close to the end.

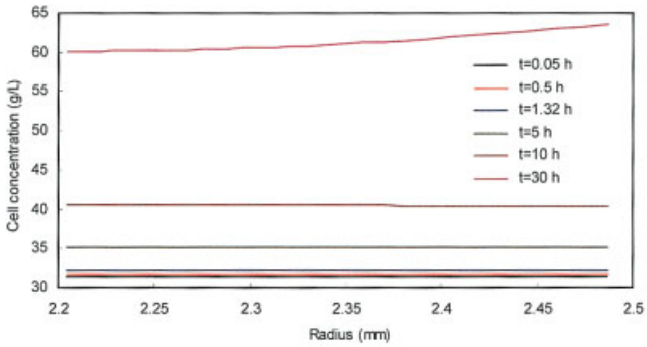

Figure 13. Radius course of the changes of cell concentration within the surface diffusion-reaction layer of the cell-immobilized polyurethane foams at different time points of batch phenol biodegradation in fermentor ($C_{S,0}$ = 1600 mg/L).

[Color figure can be viewed in the online issue, which is available at www.interscience.wiley.com.]

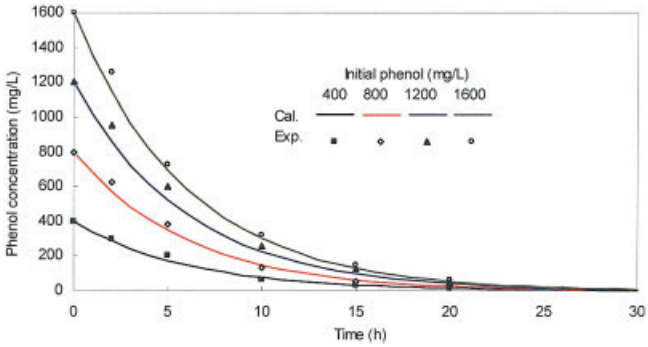

Figure 14. Time course of the changes of phenol concentration in the main liquid phase at different initial phenol concentrations of batch phenol biodegradation in fermentor.

[Color figure can be viewed in the online issue, which is available at www.interscience.wiley.com.]

The main liquid phase

Figure 14 shows the comparison between model predictions and experimentally measured phenol concentration at different initial phenol concentrations in the main liquid phase. It can be seen that the duration of the reduction time increases as the initial phenol concentration increases. For every different initial phenol concentration, the reduction rates of the first several hours are much higher than those of the last several hours. The good agreement between the simulated results and the experimental data verifies the good application of the proposed model ($R^2 = 0.99$).

Conclusions

Intrinsic kinetic parameters for cell growth and phenol biodegradation by *Alcaligenes faecalis* were determined based on the experimental data of phenol biodegradation obtained in shaking flasks.

Batch phenol biodegradation experiments were carried out in a 7.5 L fermentor to understand the dynamic behaviors of such processes by the immobilized *Alcaligenes faecalis* in polyurethane foams. A double-layer reaction-diffusion model was developed to describe the batch phenol biodegradation process. The variations of phenol concentrations against time and radial position within the inner diffusion layer and the surface diffusion-reaction layer of the cell-immobilized polyurethane foams, as well as the variation of phenol concentration against time in the main liquid phase at different initial phenol concentrations, were simulated by the proposed model and analyzed in detail. Phenol concentration experienced a peak in each of the two layers within the cell-immobilized polyurethane foams at the beginning of the process and then started to decrease to almost zero after 30 hours, while in the main liquid phase phenol concentration decreased downward all the way as time passed. The distribution of phenol concentrations along the radius course within the two layers of the cell-immobilized polyurethane foams exhibited a heterogeneous nature. To explain that, the interrelationship of phenol diffusion within the cell-immobilized polyurethane foams and mass transfer from the main liquid phase to the surface of the cell-immobilized polyurethane foams was analyzed and then a Biot number was provided.

Also, the time and radius course of the change of cell concentrations within the surface diffusion-reaction layer of the cell-immobilized polyurethane foams at different initial phenol concentrations was also simulated by the proposed model and discussed. The immobilized *Alcaligenes faecalis* in polyurethane foams grew with time course until reaching a platform when phenol was almost exhausted. The radius distribution of cell concentration experienced a turning point as the phenol biodegradation process proceeded.

The good agreement between the theoretical simulations by the proposed double-layer reaction-diffusion model and the experimental measured data of phenol biodegradation at time course in the main liquid phase indicated a general application ability of the proposed model for predicting batch phenol biodegradation with immobilized *Alcaligenes faecalis* in polyurethane foams.

Acknowledgments

The authors wish to acknowledge the financial support provided by the Key National Natural Science Foundation of China (No. 20336030), Key Natural Science Foundation of Tianjin (No. 05YFJZJC 00500), Program for New Century Excellent Talents in University, and Program for Changjiang Scholars and Innovative Research Team in University.

Notation

A = growth associated constant for phenol consumption, g phenol/g biomass
α = surface area per unit volume of the cell-immobilized polyurethane foams ($\alpha = 3/R$), m^{-1}
B = non-growth associated constant for phenol consumption, g phenol/g biomass·h
Bi = Biot number ($Bi = K_{L,S}R/D_{S,1}$), dimensionless
C = solute concentration, mg/L
$\overline{C_{X\,0}}$ = experimentally determined average cell density in the cell-immobilized polyurethane foams, mg/L
D = diffusion coefficient, m^2/s
d_P = mean particle diameter, m
$K_{L,S}$ = liquid-solid mass transfer coefficient, m/s
K_i = inhibition coefficient, mg/L
K_S = saturation constant, mg/L
m = maintenance energy coefficient, h^{-1}
R = equivalent radius of cell-immobilized polyurethane foams, m
r = radial distance coordinate, m
t = time, h
$Y_{P/S}$ = product yield coefficient, g product/g phenol
$Y_{X/S}$ = biomass yield coefficient, g biomass/g phenol

Greek letters

α = growth associated constant for product formation, g product/g biomass
β = non-growth associated constant for product formation, g product/g biomass·h
γ = rate of reaction, g/L·h
ε = solid loading, dimensionless
μ = liquid viscosity, Pa·s
μ_S = specific degradation rate ($\mu_S = (1/C_X)(dC_S/dt)$), h^{-1}
μ_X = specific growth rate ($\mu_X = (1/C_X)(dC_X/dt)$), h^{-1}
μ_{max} = maximum specific growth rate, h^{-1}
ρ = liquid density, kg/m^3
$\Delta\rho$ = density difference between the solid and liquid phases, kg/m^3

Subscripts

0 = initial condition
1 = inner diffusion layer of cell-immobilized polyurethane foams
2 = surface diffusion-reaction layer of cell-immobilized polyurethane foams

3 = main liquid phase (broth)
L = liquid
P = product
S = substrate, phenol
X = biomass

Literature Cited

1. Alexievaa Z, Gerginova M, Zlateva P, Peneva N. Comparison of growth kinetics and phenol metabolizing enzymes of *Trichosporon cutaneum* R57 and mutants with modified degradation abilities. *Enzyme and Microbial Technology.* 2004;34:242-247.
2. Kumaran P, Paruchuri YL. Kinetics of phenol biotransformation. *Water Res.* 1997;31:11-22.
3. Lannouette KH. Treatment of phenolic wastes. *Chem Eng.* 1977;84: 99-106.
4. Bandyopadhyay K, Das D. Kinetics of phenol degradation using *Pseudomonas putida* MTCC 1194. *Bioprocess Eng.* 1998;18:373-377.
5. Buitrón G, González A, López-Marín LM. Biodegradation of phenolic compounds by an acclimated activated sludge and isolated bacteria. *Water Sci Technol.* 1998;37:371-378.
6. Topalova Y, Dimkov R, Ivanov I, Sergieva S, Arsov R. Ortho-nitrophenol removal in two types activated sludge: the role of microbiological and enzymological adaptation. *Biotechnology and Bioengineering.* 1998;12:91-95.
7. Wael SE, Mohamed K, Ibrahim MA, Fawkia E, Naoya O, Hiroshi S, Akikazu A. Isolation and identification of a novel strain of the genus ochrobactrum with phenol-degrading activity. *J of Bioscience and Bioengineering.* 2003;96:310-312.
8. Chung TP, Tseng HY, Juang RS. Mass transfer effect and intermediate detection for phenol degradation in immobilized *Psendomonas putida* systems. *Process Biochemistry.* 2003;38:1497-1507.
9. Bayley RC, Barbour G. The degradation of aromatic compounds by meta and gentisate pathways; biochemistry and regulation. In: Gibson DT (Ed). *Microbial Degradation of Organic Compounds*. New York: Dekker; 1984:253-294.
10. Bandhopadhyay K. Microbial degradation of phenolic waste. PhD Thesis, IIT Kharagpur, India, 1997.
11. Pai SL, Hsu YL, Chong NM, Sheu CS, Chen CH. Continuous degradation of phenol by *Rhodococcus* sp. immobilized on granular activated carbon and in calcium alginate. *Bioresource Technology.* 1995; 51:37-42.
12. Chen KC, Lin YH, Chen WH, Liu YC. Degradation of phenol by PAA-immobilized *Candida tropicalis. Enzyme and Microbial Technology.* 2002;31:490-497.
13. Quan XC, Shi HC, Zhang YM, Wang JL, Qian Y. Biodegradation of 2, 4-dichlorophenol and phenol in an airlift inner-loop bioreactor immobilized with *Achromobacter* sp. *Separation and Purification Technol.* 2004;34:97-103.
14. Erhan E, Yer E, Akay G, Keskinler B, Keskinler D. Phenol degradation in a fixed-bed bioreactor using micro-cellular polymer immobilized *Pseudononas syringae*. *J of Chem Technol and Biotechnology.* 2004;79:195-206.
15. Akay G, Erhan E, Keskinler B. Bioprocess intensification in flow through micro-reactors with immobilized bacteria. *Bioengineering & Biotechnology.* 2005;90:180-190.
16. Banerjee I, Jayant M, Modak K, Bandopadhyay K, Das D, Maiti BR. Mathematical model for evaluation of mass transfer limitations in phenol biodegradation by immobilized *Pseudomonas putida*. *J of Biotechnology.* 2001;87:211-223.
17. Léonard D, Lindley ND. Growth of Ralstonia eutropha on inhibitory concentrations of phenol: diminished growth can be attributed to hydrophobic perturbation of phenol hydroxylase activity. *Enzyme and Microbial Technology.* 1999;25:271-277.
18. Kibret M, Somitsch W, Robra KH. Characterization of a phenol degrading mixed population by enzyme assay. *Water Res.* 2000;34: 1127-1134.
19. Brooks CA, Cramer SM. Solute affinity in ion-exchange displacement chromatography. *Chem Eng Sci.* 1996;51:3847-3860.
20. Monteiro ÁAMG, Boaventura RAR, Rodirgues AE. Phenol biodegradation by *Pseudomonas putida* DSM 548 in a batch reactor. *Biochemical Eng J.* 2000;6:45-49.
21. Hao OJ, Kim MH, Seagren EA, Kim H. Kinetics of phenol and chlorophenol utilization by *Acinetobacter species. Chemosphere.* 2002;46:797-807.
22. Feitkenhauer H, Schnicke S, Müller R, Märkl H. Kinetic parameters of continuous cultures of Bacillus *thermoleovorans sp.* A2 degrading phenol at 65°C. *J of Biotechnology.* 2003;103:129-135.
23. Oyaas J, Storro I, Svendsen H, Levine DW. The effective diffusion coefficients and the distribution constant for small molecules in calcium-alginate gel beads. *Biotechnology and Bioengineering.* 1995;47: 492-500.
24. Wang H, Seki M, Furusaki S. Mathematical model for analysis of mass transfer for immobilized cells in lactic acid fermentation. *Biotechnology Progress.* 1995;11:558-564.
25. Zhang SP, Sun Y. Ionic strength dependence of protein adsorption to dye-ligand adsorbents. *AIChE J.* 2002;48:178-186.
26. Escobedo J, Mansoori GA. Asphaltene and other heavy-organic particle deposition during transfer and production operations. *Proc-SPE Ann Tech Conf and Exhibition*. 1995;Volume Pi:343-358.

Manuscript received Feb. 3, 2005, and revision received Aug. 14, 2005, and final revision received Nov. 4, 2005.